Arabian Journal for Science and Engineering
https://doi.org/10.1007/s13369-023-08652-5

RESEARCH ARTICLE-CHEMISTRY

The Photocatalytic Performance of Ag /TiO_2/Nylon 6/PMMA System

Kinyas Polat[1] · **Elif Ant Bursalı**[2] · **Mürüvvet Yurdakoç**[2] · **Kadir Yurdakoç**[2]

Received: 13 July 2023 / Accepted: 18 December 2023
© The Author(s) 2024

Abstract
Herein, Ag/TiO_2/Nylon 6/PMMA catalyst system was developed, and its photocatalytic properties were fully analyzed. XRD, SEM, EDS, and PL analyses were carried out to get information on crystal structure, micromorphology, elemental composition, and band gap energy. Photocatalytic degradation was followed by UV–vis spectrophotometry. The band gap of the catalyst was found to be between 2.51 and 3.1 eV. Up to 80% degradation was achieved under UV light irradiation. No bulk adsorption was observed, which means that the reaction was completely carried by the photocatalytic process. pH 3 value was determined to be suitable for a high rate. Reaction kinetic was determined to be matched with the first-order rate law. The newly developed polymer blend matrix system here may have broad application prospects in the remediation of water resources.

Keywords Ag/TiO_2 · Photocatalysis · UV irradiation · Nylon 6/PMMA blend · Dip coating

1 Introduction

Including the various approaches to removing dye molecules, heterogeneous photocatalysis is gaining importance in scientific research allowing major dye groups and their associated decomposition intermediates and by-products to degrade, mineralize, and eventually be almost eliminated. Most photocatalytic materials have high band gaps; therefore, UV rays can only excite them. TiO_2 is one of those materials and there is a high band gap (3.0 eV for the rutile phase, 3.2 eV for the anatase phase) thus a high recombination rate exists due to poor separation efficiency between photogenerated electron–hole pairs [1, 2]. However, doping has been developed to efficiently overcome this limitation to exploit the low-cost advantages of this abundant natural material. Moreover, TiO_2 is a green chemical. Indeed, it is a food additive [3].

The photocatalytic activity of TiO_2 is based on reactive oxygens species generated such as hydroxyl radicals during UV irradiation. They completely degrade many organic contaminants such as chlorinated compounds, pesticides, dyes, etc. without being structurally affected in terms of chemical stability [4]. As noted above, doping is the gold key to boosting the efficiency of these processes through the narrowing of the band gap and is being done by several methods such as self-doping, ion doping, rare earth metal doping, transition metal doping [1, 5, 6, 7]. Noble metal doping is the other choice for enhancing the efficiency of TiO_2; it was shown that noble metal (Pt and Ag) doped TiO_2 effectively degraded the dichloroacetic acid (DCA) through the hydroxyl radicals (•OH) from the transformation of superoxide radicals (O_2•$^-$). It was also shown that •OH radicals are responsible for the degradation of DCA in the case of neat TiO_2. They were generated from positively charged holes leading to a different pathway. Pt and Ag as noble metal doping materials achieved 100 and 79.3% removal of DCA [8]. In another study, Ag nanoparticles and TiO_2 were prepared as composite films by sol–gel and dip-coating method for the catalytic degradation of mordant orange dye. In the study, a catalytic efficiency of up to 60.61% was found by the role of •OH radicals under UV-A irradiation [9]. The study on photocatalytic activity of Ag/Au doped TiO_2 with the presence of reduced graphene oxide (rGO) revealed that methylene blue degradation rate was in the order Ag–Au/rGO/TiO_2 > Au/rGO/TiO_2 > Ag/rGO/TiO_2 under visible light irradiation. The rate increase was concluded due to the low fermi energy level of these formulations [10]. Biochar was added to TiO_2/Ag mixture as a ternary

✉ Kinyas Polat
kpolat@sinop.edu.tr

1 Faculty of Engineering and Architecture, Department of Metallurgical and Materials Science Engineering, Sinop University, 57000 Sinop, Turkey

2 Faculty of Science, Department of Chemistry, Dokuz Eylül University, 35390 Izmir, Turkey

Published online: 23 February 2024

ingredient and was reported to have up to 97.48% photocatalytic efficiency for the degradation and mineralization of methyl orange [11]. In the study, it was shown that Ag and TiO_2 acted as electron donors while biochar was an electron acceptor. It was also found that photocatalytic reaction was enhanced under low pH values rather than the neutral or basic pH ranges. Besides noble metal doping strategies, immobilization techniques are another way to improve photocatalytic efficiency through enhanced adsorption on the catalysis surface. The study where the Ag/TiO_2 was immobilized on natural fibers using hexadecyl-trimethyl-ammonium bromide (CTAB) revealed that degradation was completed within 2 h at 40 °C [12]. Another strategy worth saying is molecular imprinting technology (MIT), which uses the combination of target pollutants and catalysts materials and then specific techniques to elute imprinted molecules to get molecular imprinted polymers (MIPs) or inorganic molecular imprinted (MI) products [13–15]. Noble metal-doped TiO_2 formulations within a polymer matrix has been increasingly gaining attention recently due to advantage introduced by polymers such as easy immobilization on a variety of different surface like glass and nano-structure formation ability. An example of this kind of strategy was Ag/TiO_2 in polyvinyl alcohol (PVA) electro-spun mats utilized as photocatalyst for the removal of methylene blue under visible light irradiation [16]. Ag/TiO_2/PDMS composites were applied on a cotton fabric as a recyclable water purification material with self-cleaning properties through superhydrophobic Ag/TiO_2/PDMS photocatalyst in which adhesion and super hydrophobicity is achieved by poly(dimethylsiloxane) (PDMS) [17]. TiO_2 nanoparticles smaller than 4 nm were coated on polymethylmethacrylate (PMMA) for photocatalysis of different dyes such as methylene blue, methyl orange, rhodamine B, and 80% of removal efficiency was observed. In the study [18], PMMA substrate was chosen due to flexibility and cheapness. Polyamide 6 (Nylon 6) was used as a coating agent for nano-sized TiO_2 production by using a precipitation technique in which PA6 powders with a particle size of 20–90 μm were obtained. The study showed that nanoparticles (Nylon 6 coated TiO_2) were a potential material for laser powder bed diffusion manufacturing technique. However, no photocatalytic performance was tested [19]. Photocatalyst systems utilizing the versatile properties of polymers have been an area that is not much investigated thus a few studies are present in the literature.

In the present study, Ag/TiO_2 powders were embedded in a PMMA/Nylon 6 matrix for the first time which was then dip coated to produce a surface-coating photocatalyst material on glass substrates. Ag particles were obtained by using a half-cell displacement reaction of silver and copper ions. The photocatalytic activity was tested against Remazol blue dye degradation. This study may help understand the importance of polymer mixtures in finding a suitable support or carrier matrix material for powder-type catalysts. Another important advantage of the study is that the prepared catalyst does not need filtration due to the immobilization of the material on glass slide thus eliminating the extra steps in the process to remove the catalyst residue from the solution.

2 Experimental Section

2.1 Materials

TiO_2 (P25) was supplied from Degussa: Hulls. Silver Nitrate (Product code 85,228), Nylon 6 (product code 181,110), and PMMA (Product code 445746) were purchased from Sigma-Aldrich. Copper foil (Product code 46,365) obtained from Alfa Aesar. Remazol Blue dye was obtained from Sigma-Aldrich (Product Code R8001-25G).

2.2 Synthesis of Silver Powders

Silver powders were obtained by utilizing the commonly known redox reaction between copper metal and silver ions. Copper metal in the form of high-purity foil was cut into 25 cm^2 total area rectangle shapes suitable for immersing into a 100 mL beaker. Before use, the surfaces of the foils were wiped with formic acid thoroughly to remove the organic and other species then cleaned up with water and washed with isopropyl alcohol then allowed to dry at room temperature. For the redox reaction 5 g silver nitrate was dissolved in 100 mL of deionized water and copper foils were immersed into the silver nitrate solution until all the copper foils were dissolved as copper ions. At the end of the reaction, silver metals were precipitated at the bottom of the beaker. The silver precipitate was then filtered, washed with water, and dried at 70 °C for 5 h.

2.3 Preparation of the Photocatalyst

2.5 g of PMMA and Nylon 6 solid pellets were weighed and added into 50 mL of formic acid. After 24 h, dissolution was completed at room temperature. Polymers blend was obtained as a transparent liquid solution. Firstly, the silver powder ratio in the catalyst was fixed at 0.25 g at all formulations. TiO_2 was added into the polymer blend at increasing amounts from 0.25 g up to 1 g with 0.25 g increase in each. 5 mL of polymer blend solution was used in all formulations. Therefore, four different samples were obtained. To illustrate, the sample included 0.25 g Ag, 0.25 g TiO_2, and 5 mL of polymer blend solution was named *poly 1*. The sample containing 0.25 g Ag, 0.50 g TiO_2, and 5 mL of polymer blend solution was named *poly 2* etc. In order to compare the effect of silver, a sample that does not contain silver was prepared and

named *poly 5*. Polymer solution and catalyst powder mixing was achieved by mini hand mixer for 1 h. Microscope glass slides were wiped with formic acid, cleaned by water thoroughly and allowed to dry. Catalyst coating onto these glass substrates was carried out by dip coating method that the cleaned glass simply immersed into the catalyst solution and dried at 70 °C for 5 h. One side of the catalyst on the slide was scraped. The amount of catalyst on one side of the slides weighted was 0.011 g for poly 1, 0.020 g for poly 2, 0.032 g for poly 3, 0.048 g for poly 4, 0.050 g for poly 5. (The weighted amounts has approximately ± 0.05 g error.)

2.4 Photocatalytic Degradation

Photocatalytic performance of the samples was carried out as the slide was horizontally lied at the bottom of a suitable transparent glass container vertically positioned against the UV lamp (Osram 300 W). 100 mL of Remazol blue solution was added into the container. A small portion of irradiated solution was taken at varying intervals and absorption was measured by UV–vis spectrophotometer. Degradation rates were evaluated according to Eq. 1.

$$\eta(\%) = \left[\frac{(C_0 - \mathrm{C})}{C_0}\right] \times 100 \tag{1}$$

In the equation, η represents the degradation rate, C_0 represents the absorbance of the stock solution, and C represents the absorbance at a certain moment. Important parameters such as pH, catalyst amount, dye concentration was also evaluated to find the optimum conditions for photocatalysis. To be sure that no contribution occurs from photolysis or adsorption, blank and dark experiments were also carried out.

2.5 Photoluminescence Spectra

The band gap energy of the catalyst was found by using the photoluminescence spectroscopy (PL) technique. From the excitation and emission spectrum, the band gap energy of the catalyst was calculated according to Eq. 2 given below.

$$E_g = h\nu = h\frac{c}{\lambda} \tag{2}$$

where E_g is the band gap energy, h is the Planck constant (6.625×10^{-34} Js), ν is frequency, c is the speed of light (2.998×10^8 ms^{-1}). If 1 eV is taken as 1.602×10^{-19} J, 1nm as 10^{-9} m, then this equation is converted to the simplified form as given in Eq. 3.

$$E_g = \frac{1240}{\lambda} \tag{3}$$

Equation 3 gives the band gap energy in eV unit.

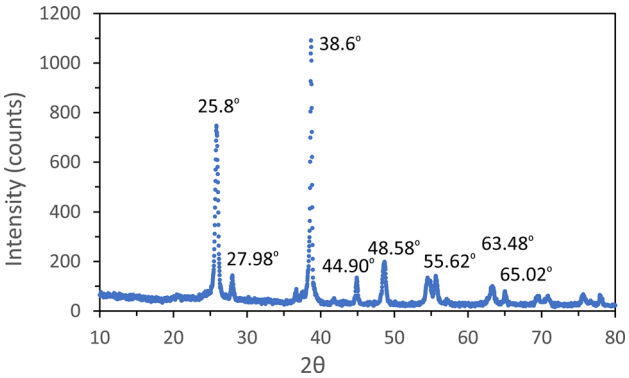


Fig. 1 XRD pattern of Ag/TiO_2/Nylon 6/PMMA

2.6 Characterization

X-ray powder diffractometer was used to determine the phase of the powder (Panalytical Empyrean XRD). An ultraviolet–visible spectrophotometer was used to determine the light absorption properties of the samples (UV–Vis, Shimadzu UV 1800). Scanning electron microscope (SEM (FEI QUANTA 250 FEG)) was used to determine the surface properties of the catalyst and elemental analysis was carried out with energy dispersive spectra (EDS) detector (Oxford Aztec). Band gap of the catalyst was measured by using FLSP920 photoluminescence spectrometer (PL).

3 Result and Discussion

3.1 XRD Analysis

As shown in Fig. 1, the XRD patterns show that the diffraction peaks of the composite catalyst *poly 3* as a representative sample. In the diffractogram, reflections of TiO_2 are in harmony with the anatase standard (JCPDS card No. 21-1272). The diffraction at 25.80°, 38.60°, 48.58°, 55.62°, and 65.02° equal angles correspond to the diffraction peaks of (1 0 1), (1 1 1), (2 0 0), (2 0 4) planes. The peak at 38.60° is due to the sum of the Ag (1 1 1) [20] and TiO_2 (1 1 1) reflections. According to the JCPDS file No. 04–0783 for Ag, the diffraction peaks at 44.90°, 63.08° corresponds to the (2 0 0) and (2 2 0) planes. Also, a small reflection was observed originating from the rutile phase TiO_2 at 27.98° corresponding to (1 1 0) plane (JCPDS card No. 21-1276). No net diffraction pattern belongs to the polymer blend was encountered due to the amorphous nature of the polymers and small portion in the catalyst formulations.

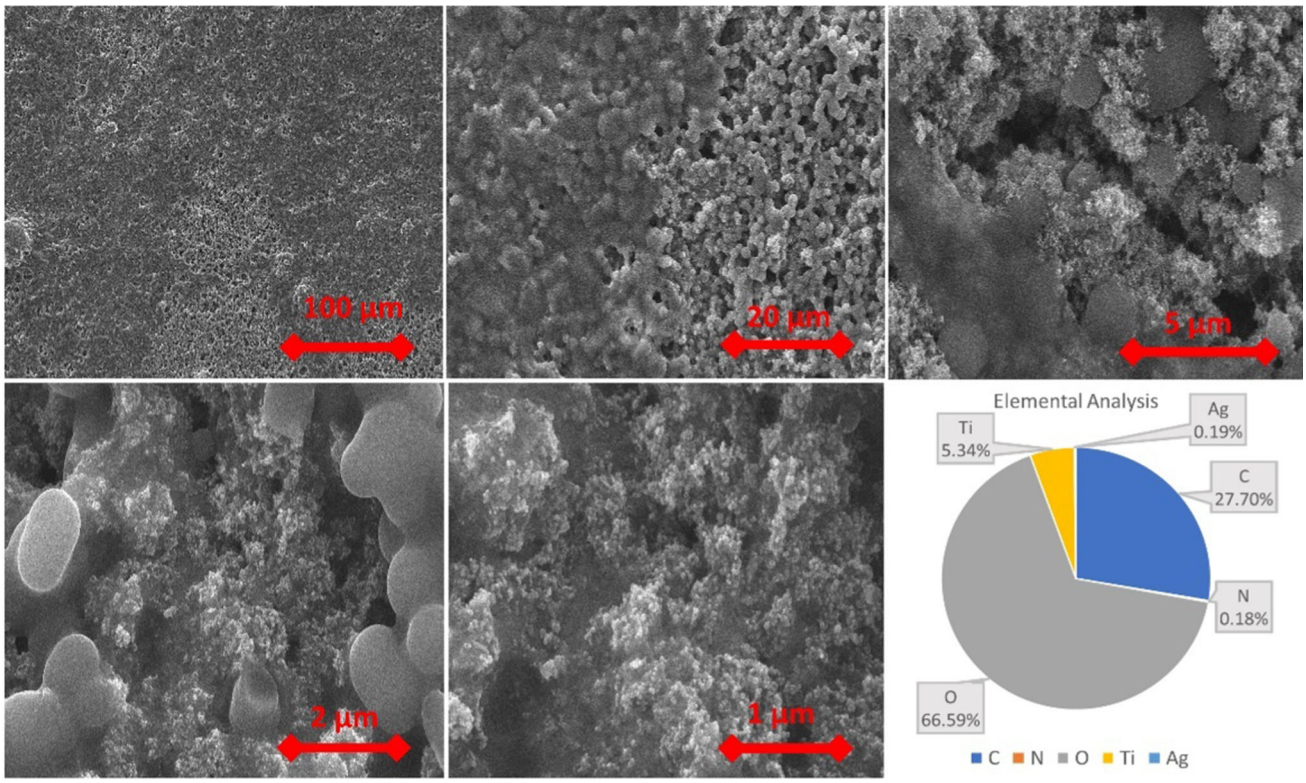


Fig. 2 SEM image and Elemental analysis chart of Ag/TiO_2/Nylon 6/PMMA composite

3.2 SEM Analysis

SEM images shown in Fig. 2 are observed with 10 kV acceleration voltage and varying magnification values between 5 and 10k. It shows first an apparent roughness on the surface. As going from 100 to 1 µm in the images, well-immobilized TiO_2 particles become clearer. Images of *poly 3* as a representative sample have homogeneously distributed white slits and holes that could more probably be generated by the splitting of hydrophobic PMMA chains due to the small water adsorption characteristic of Nylon 6, which is an advantage for the creation of active sides during photocatalysis. Indeed, this was an expected situation, and the main motivation of the study was to bring PMMA and Nylon 6 polymers together as a matrix or immobilization material. In other words, a potential hindering or encapsulation effect toward photocatalytic activity by polymer matrix was eliminated by the mentioned separate character of these polymers. Semiqualitative elemental analysis by EDS detector was explained as a graph in Fig. 2. Polymer existence is understood from carbon atom percentage while TiO_2 and Ag seen from Ti, Ag, and oxygen content. Oxygen content also comes from the carboxyl groups in both polymers.

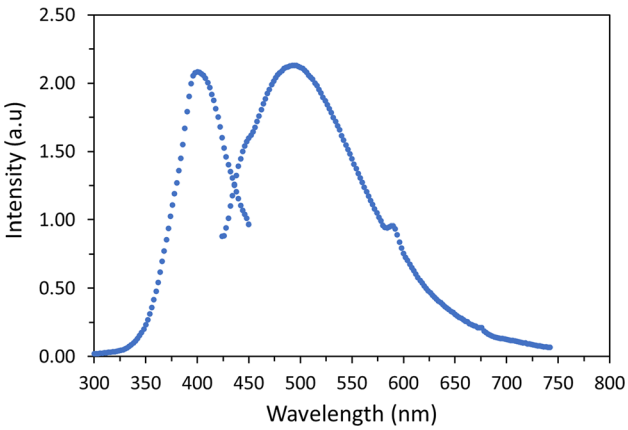


Fig. 3 PL excitation and emission spectra of Ag/TiO_2/Nylon 6/PMMA

3.3 PL Analysis

PL spectra of Ag/TiO_2/Nylon 6/PMMA films were collected by excitation at 400 nm are given in Fig. 3. The peak wavelength of the excitation spectrum was observed at 400 nm which corresponds to 3.1 eV. This energy was absorbed by the catalyst to excite its valence electrons to the conduction band. It can be seen from the emission spectra, which is given in Fig. 3 that a broad emission band is formed from 425 to 750 nm, and there is one distinct emission peak placed at

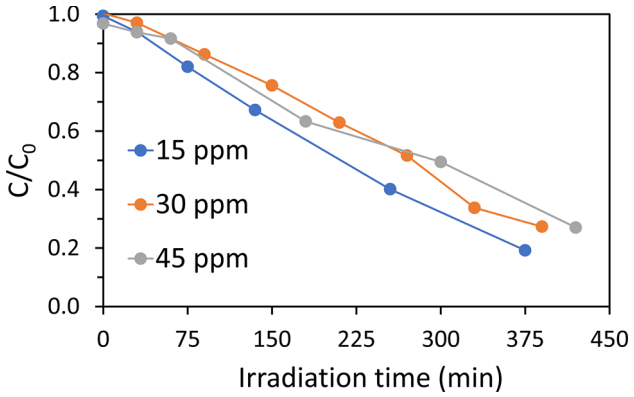


Fig. 4 Degradation rate depending on the Remazol blue concentration

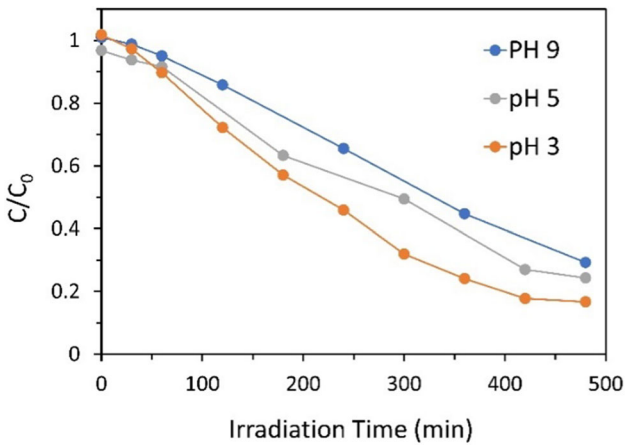


Fig. 5 Degradation rate depending on pH of Remazol blue solution

494 nm. This strong luminescence indicates the presence of defects stemming from incorporated Ag particles in TiO_2 and oxygen vacancies (VO) on the TiO_2 surface [21]. These defects change or shift the energy levels in TiO_2, enabling the sub-band electronic transitions that cause the absorption of photons in the visible part of the electromagnetic spectrum. Emission spectra suggests that the band gap energy is 2.51 eV. From this result, it can be said that band gap energy of the catalyst should be between 2.51 and 3.1 eV. Thus, a UV dominated activity exists for the catalyst system introduced here.

3.4 Photocatalytic Performance

Photocatalytic activity is affected heavily by the transparency of the dye solution. If a dye solution hinders the irradiation onto the catalyst surface, then the photocatalytic reaction becomes slower or no reaction may be observed. In other words, transparency limits the usability of photocatalysts. To determine the usability range in the Remazol blue solution degradation rate against dye concentration was measured first and plotted in Fig. 4. 45 ppm dye concentration was found to be the highest limit for transparency of light, and 15 ppm is the lowest one. To decide this, UV–vis calibration linearity was used according to Brag's law. Outside the 15–45 ppm range, calibration curve was not a linear line. According to Fig. 4, reaction rate gets slower in going from 15 to 45 ppm but not much difference was seen practically. It took 420 min for the 45 ppm, 390 min for the 30 ppm, and 375 min for the 15 ppm for the reaction to completely be finished. 70% degradation was achieved for 45 and 30 ppm, and 80% was achieved for 15 ppm. It was shown that at the lowest transparency limit (45 ppm) where the UV light has difficulty penetrating the solution, 70% degradation was possible. If the transparency is high as in the 15-ppm sample or for possible dilute solutions, 80% or more degradation values can be achieved.

Another important factor that influences the performance is the acidity of the solution. As dyes can be used in different industrial processes, performance evaluation in different pH values is necessary. Therefore, three different values were selected, and photocatalytic activity was tested and plotted as given in Fig. 5. A relatively high reactivity at acidic pH was observed as compared to other pH values. The reason for the preference of a high rate at the acidic pH range is dependent on the surface charge of the photocatalyst [22]. It can change the adsorption properties of the dye. Electrostatic interactions, solvent molecules, and charged molecules formed during photocatalytic reaction are all dependent on the pH of the solution [23]. If the photocatalyst tends to become positively charged then a high rate will be observed in acidic pH values, otherwise basic conditions will be favored. Surface of the Ag/TiO_2/Nylon 6/PMMA photocatalyst becomes positively charged when the pH is adjusted to the acidic region due to the protonated OH groups of TiO_2 and NH groups of the Nylon 6 chains. As the sulphonic acid groups of the dye molecule are negatively charged, they are attracted to the positively charged regions of the catalyst which increases the adsorption and consequently rate of degradation. This mechanism is briefly depicted in the scheme given in Fig. 6.

45 ppm dye concentration and pH 3 were selected as a starting point for identification of overall catalytic performance. To be sure that no contribution comes from the photolysis and bulk adsorption, blank and dark experiments were realized. Photolysis is the process in which only irradiation is responsible for degrading the molecules without a catalyst. Radiation-sensitive molecules are especially degraded upon interaction with light. To eliminate the probability of photolysis a dye solution is waited under UV irradiation for the longest time required for the reaction with catalyst. Bulk adsorption by the catalyst material is another cause for decolorization or removal of dye from the solution without going into the photocatalytic reaction.

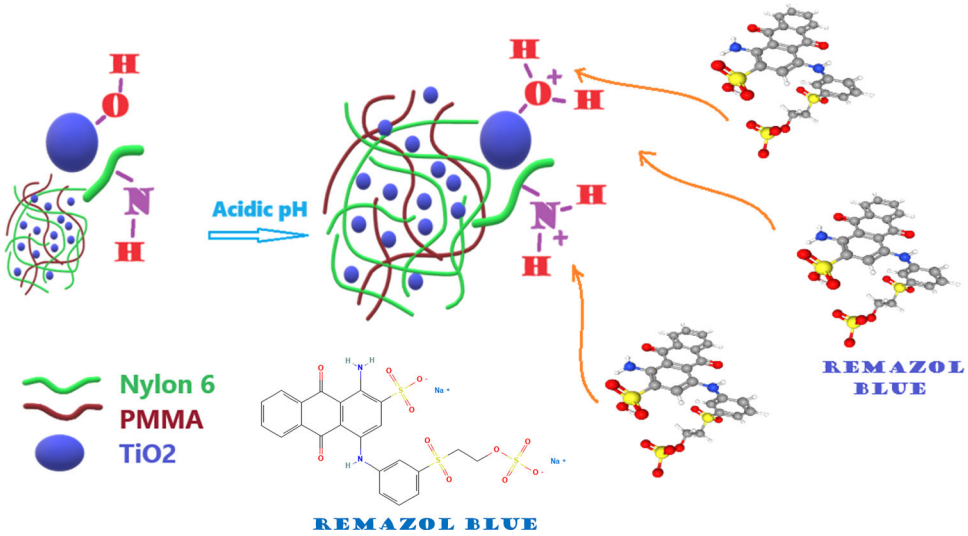


Fig. 6 Effect of acidic pH on degradation

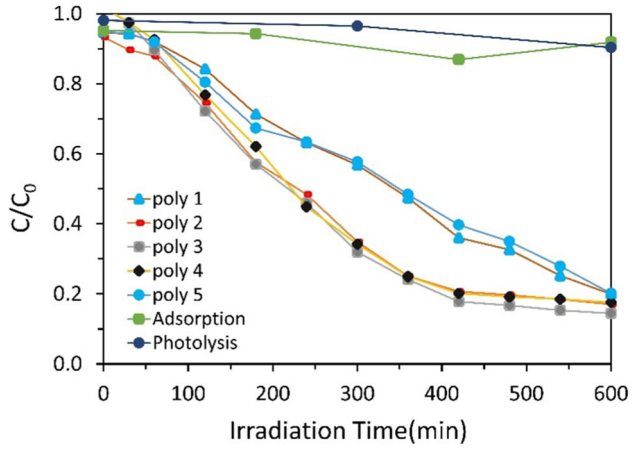


Fig. 7 Degradation rate comparison of 45 ppm Remazol blue at pH 3 by all catalysis formulations

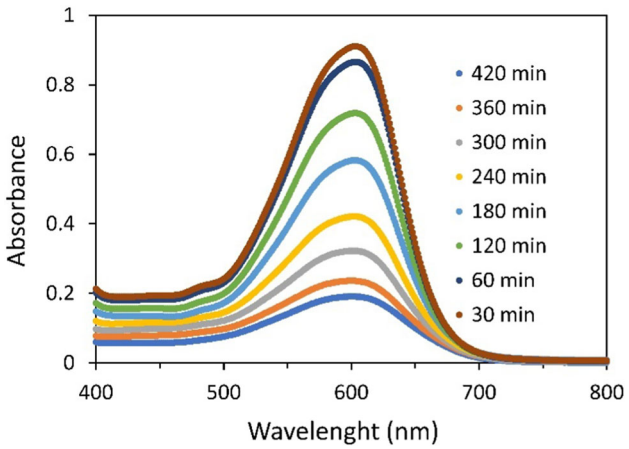


Fig. 8 Degradation of Remazol blue at its wavelength max

To determine whether the catalyst material contributes to the bulk adsorption removal, catalyst material was immersed in a dye solution saved in dark environment. Results of both photolysis and dark experiments were plotted against time and given in Fig. 7. As understood from Fig. 7, dye degradation is clearly carried out by photocatalytic processes. Figure 7 also shows that *poly 1* has the same degradation capability as *poly 5* having no Ag content. This means that rate acceleration effect introduced by Ag is equal to the one obtained by TiO_2 increase. Catalysts named *poly 2*, *poly 3*, and *poly 4* have the same degradation rate but higher than *poly 1* and *poly 5*. It is considered that above the amount of catalyst used in *poly 1*, synergistic contribution of Ag particles to the reaction rate masks the effect of TiO_2 and no net difference is obtained. Overall degradation rate of the catalyst reaches up to 80%. Gradual degradation of Remazol blue dye at its wavelength max between 400 and 800 nm is given in Fig. 8.

As to the reaction mechanism, it can be said that the main degradation takes place through the hydroxyl radicals (•OH) from the transformation of superoxide radicals ($O_2^{\bullet -}$). In the acidic pH values, the formation of hydroxyl radicals is boosted. Hydroxyl radicals attack the double bonds which are more sensitive molecular parts of Remazol dye. By the attack of hydroxyl radical, the dye molecule divides into two parts first and then gradually into smaller compounds like CO_2, H_2O, CO_X, NO_X by the bond breakages on the double bonds [24].

3.5 Photocatalytic Reaction Kinetics

The kinetic model of degradation was also analyzed and found that first order kinetics is applicable to the reaction (Fig. 9). First-order kinetic is defined as in Eq. 4.

$$\ln[C] = \ln[C_0] - kt \tag{4}$$

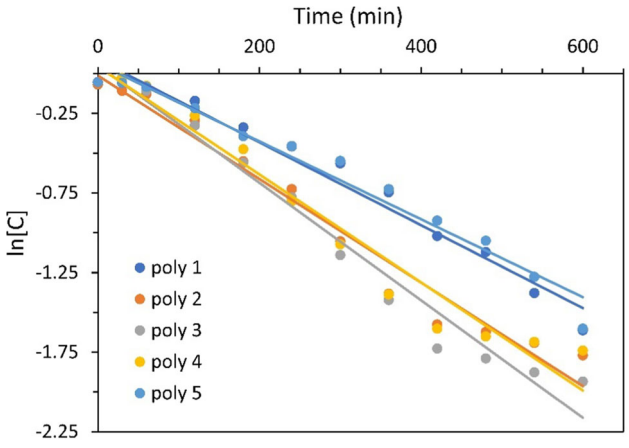


Fig. 9 First-order kinetic model of Remazol blue

Table 1 Kinetic parameters of photocatalytic reaction

Catalyst	Rate constant (k/s^{-1})	R^2
Poly 1	0.0026	0.97
Poly 2	0.0033	0.97
Poly 3	0.0037	0.97
Poly 4	0.0034	0.96
Poly 5	0.0024	0.97

where C, C_0,k, t is the dye concentration at any moment, initial concentration of the dye, reaction rate constant, and time, respectively. A linear graph of t versus $ln\ C$ demonstrates that first order kinetics is the case. The linearity of the graph is determined by the R^2 values. Results of kinetic assessment are given in Fig. 9. Reaction rate constants and R^2 values are summarized in the following Table 1. R^2 values were found to be 0.97 and linearity suggests that more probably reaction follows the first-order kinetic pathway and concentration dependent. In other words, rate increase or decrease is related to the available dye molecules on active sides of photocatalyst surface at any moment. As seen in the table rate constants of poly 1 and 5 are smaller than others as mentioned earlier. Consistent values of reaction rate constants proves again that first-order kinetic model are very well fits the available pathway.

4 Conclusions

A new type of polymer blend (Nylon 6 and PMMA) was applied to the Ag/TiO_2 powder catalyst system as an immobilizing agent or carrier. Hydrophobicity of PMMA and little water adsorption capability of Nylon 6 make out a slits and hole dominant micro morphology as shown by SEM observation. XRD results suggested that the main TiO_2 crystal structure was the photoactive anatase phase. Synergistic rate increase introduced by Ag was so important that the effect of an increase in TiO_2 content was almost masked in poly 2, poly 3, and poly 4 named samples. PL spectra results suggested that the band gap of the catalyst should be between 2.51 and 3.1 eV. Successful photocatalytic degradation up to 80% was achieved. The first-order kinetic model fits the reaction and suggests that reaction is concentration dependent that availability of dye molecules on active sides on catalyst surface influences the rate. The catalyst system also removes the filtration step for residue removal from the medium resulting in time effective method. The present study demonstrated that the polymer blend could be a potential carrier material for powder catalyst systems.

Author contribution KP designed the study and prepared the catalyst materials and wrote the manuscript. EAB, MY, and KY carried out the photocatalytic degradation experiments. XRD, SEM, EDS, and PL performed analysis.

Funding Open access funding provided by the Scientific and Technological Research Council of Türkiye (TÜBİTAK).

Declarations

Conflict of interests The authors declare no competing interests.

Ethical approval There are no ethical issues in this article.

Consent to participate All authors agree to participate in this paper.

Consent to publish All authors agree to the publication of this paper.

Open Access This article is licensed under a Creative Commons Attribution 4.0 International License, which permits use, sharing, adaptation, distribution and reproduction in any medium or format, as long as you give appropriate credit to the original author(s) and the source, provide a link to the Creative Commons licence, and indicate if changes were made. The images or other third party material in this article are included in the article's Creative Commons licence, unless indicated otherwise in a credit line to the material. If material is not included in the article's Creative Commons licence and your intended use is not permitted by statutory regulation or exceeds the permitted use, you will need to obtain permission directly from the copyright holder. To view a copy of this licence, visit http://creativecommons.org/licenses/by/4.0/.

References

1. Yu, X.; Hou, T.; Sun, X.; Li, Y.: The influence of defects on Mo-doped TiO_2 by first-principles studies. ChemPhysChem **13**, 1514–1521 (2012). https://doi.org/10.1002/cphc.201101012
2. Mudhoo, A.; Paliya, S.; Goswami, P., et al.: Fabrication, functionalization and performance of doped photocatalysts for dye degradation and mineralization: a review. Environ. Chem. Lett. **18**, 1825–1903 (2020). https://doi.org/10.1007/s10311-020-01045-2
3. Boutillier, S.; Fourmentin, S.; Laperche, B.: History of titanium dioxide regulation as a food additive: a review. Environ. Chem.

Lett. **20**, 1017–1033 (2022). https://doi.org/10.1007/s10311-021-01360-2
4. Kumar, L.; Ragunathan, V.; Chugh, M.; Bharadvaja, N.: Nanomaterials for remediation of contaminants: a review. Environ. Chem. Lett. **19**, 3139–3163 (2021). https://doi.org/10.1007/s10311-021-01212-z
5. Borlaf, M.; Colomer, M.T.; de Andrés, A., et al.: TiO_2/Eu^{3+} thin films with high photoluminescence emission prepared by electrophoretic deposition from nanoparticulate sols. Eur. J. Inorg. Chem. **2014**, 5152–5159 (2014). https://doi.org/10.1002/ejic.201402445
6. Coromelci, C.; Ignat, M.; Sacarescu, L.; Neamtu, M.: Enhanced visible light activated mesoporous titania by rare earth metal doping. Microporous Mesoporous Mater. **341**, 112072 (2022). https://doi.org/10.1016/j.micromeso.2022.112072
7. Yoon, Y.H.; Lee, S.Y.; Gwon, J.G., et al.: Transition metal-doped mesoporous TiO_2 films fabricated through cellulose nanocrystal template synthesis: studies of physicochemical, spectrophotometric properties, and photocatalytic degradation activity. Cellulose **29**, 9199–9215 (2022). https://doi.org/10.1007/s10570-022-04830-0
8. Ribao, P.; Corredor, J.; Rivero, M.J.; Ortiz, I.: Role of reactive oxygen species on the activity of noble metal-doped TiO_2 photocatalysts. J. Hazard. Mater. **372**, 45–51 (2019). https://doi.org/10.1016/j.jhazmat.2018.05.026
9. Vanlalhmingmawia, C.; Lalhriatpuia, C.; Tiwari, D.; Kim, D.-J.: Noble metal-doped TiO_2 thin films in the efficient removal of Mordant Orange-1: insights of degradation process. Environ. Sci. Pollut. Res. **29**, 51732–51743 (2022). https://doi.org/10.1007/s11356-021-17568-2
10. Khairy, M.; Kamar, E.M.; Mousa, M.A.: Photocatalytic activity of nano-sized Ag and Au metal-doped TiO_2 embedded in rGO under visible light irradiation. Mater. Sci. Eng. B **286**, 116023 (2022). https://doi.org/10.1016/j.mseb.2022.116023
11. Shan, R.; Lu, L.; Gu, J., et al.: Photocatalytic degradation of methyl orange by Ag/TiO_2/biochar composite catalysts in aqueous solutions. Mater. Sci. Semicond. Process. **114**, 105088 (2020). https://doi.org/10.1016/j.mssp.2020.105088
12. Lopes, F.C.S.M.R.; da Rocha, MGC, Bargiela P, et al.: Ag/TiO_2 photocatalyst immobilized onto modified natural fibers for photodegradation of anthracene. Chem. Eng. Sci. **227**, 115939 (2020). https://doi.org/10.1016/j.ces.2020.115939
13. Peng, D.; Li, X.; Zhang, L.; Gong, J.: Novel visible-light-responsive photoelectrochemical sensor of 2,4-dichlorophenoxyacetic acid using molecularly imprinted polymer/BiOI nanoflake arrays. Electrochem. Commun. **47**, 9–12 (2014). https://doi.org/10.1016/j.elecom.2014.07.010
14. Liu, M.; Ding, X.; Yang, Q., et al.: A pM leveled photoelectrochemical sensor for microcystin-LR based on surface molecularly imprinted TiO_2@CNTs nanostructure. J. Hazard. Mater. **331**, 309–320 (2017). https://doi.org/10.1016/j.jhazmat.2017.02.031
15. Liu, X.; Li, X.; Zhu, L.; Wang, X.: Preparation of molecularly imprinted $Ag\text{-}TiO_2$ for photocatalytic removal of ethyl paraben. Environ. Sci. Pollut. Res. **29**, 10308–10318 (2022). https://doi.org/10.1007/s11356-021-16168-4
16. Montallana, A.D.S.; Vasquez, M.R.: Fabrication of $PVA/Ag\text{-}TiO_2$ nanofiber mats for visible-light-active photocatalysis. Results Phys. **25**, 104205 (2021). https://doi.org/10.1016/j.rinp.2021.104205
17. Zhang, M.; Jiang, S.; Han, F., et al.: Recyclable, superhydrophobic and effective Ag/TiO_2@PDMS coated cotton fabric with visible-light photocatalyst for efficient water purification. Cellulose **29**, 3529–3544 (2022). https://doi.org/10.1007/s10570-022-04477-x
18. Iesalnieks, M.; Eglītis, R.; Juhna, T., et al.: Photocatalytic activity of TiO_2 coatings obtained at room temperature on a polymethyl methacrylate substrate. Int. J. Mol. Sci. **23**, 12936 (2022). https://doi.org/10.3390/ijms232112936
19. Chen P, Li Z, Liu S, et al.: Preparation of polyamide 6 and its titanium dioxide photocatalytic composite powders for laser powder bed fusion. Mater. Sci. Additive Manufact. 1 (2022).. https://doi.org/10.18063/msam.v1i3.14
20. Lanje, A.; Sharma, S.; Pode, R.: Synthesis of silver nanoparticles: a safer alternative to conventional antimicrobial and antibacterial agents. J. Chem. Pharm. Res. **2**, 478–483 (2010)
21. Liqiang, J.; Yichun, Q.; Baiqi, W., et al.: Review of photoluminescence performance of nano-sized semiconductor materials and its relationships with photocatalytic activity. Sol. Energy Mater. Sol. Cells **90**, 1773–1787 (2006). https://doi.org/10.1016/j.solmat.2005.11.007
22. Sakarkar, S.; Muthukumran, S.; Jegatheesan, V.: Factors affecting the degradation of remazol turquoise blue (RTB) dye by titanium dioxide (TiO_2) entrapped photocatalytic membrane. J. Environ. Manage. **272**, 111090 (2020). https://doi.org/10.1016/j.jenvman.2020.111090
23. Mendret, J.; Hatat-Fraile, M.; Rivallin, M.; Brosillon, S.: Influence of solution pH on the performance of photocatalytic membranes during dead-end filtration. Sep. Purif. Technol. **118**, 406–414 (2013). https://doi.org/10.1016/j.seppur.2013.07.025
24. Purnawan, C.; Wahyuningsih, S.; Aniza, O.; Sari, O.: Photocatalytic degradation of Remazol Brilliant Blue R and Remazol Yellow FG using TiO2 doped Cd Co, Mn. Bull. Chem. React. Eng. Catal. **16**, 804–815 (2021). https://doi.org/10.9767/bcrec.16.4.11423.804-815